Available online at www.sciencedirect.com
ScienceDirect
Journal of the European Ceramic Society 28 (2008) 895–899
www.elsevier.com/locate/jeurceramsoc

Synthesis of nanosized ceramic powders in a radiofrequency thermal plasma reactor

János Szépvölgyi [a,b,*], Ilona Mohai [a], Zoltán Károly [a], Loránd Gál [a]

[a] *Institute of Materials and Environmental Chemistry, Chemical Research Centre, Hungarian Academy of Sciences, Budapest, Hungary*
[b] *Research Institute of Chemical and Process Engineering, University of Pannonia, Veszprém, Hungary*

Available online 25 October 2007

Abstract

Recent results in the synthesis of nanosized ceramic powders in a radiofrequency (RF) thermal plasma reactor are presented in this paper. Two ceramic materials, namely silicon dioxide and lanthanum hexaboride were selected as models of investigations. In both cases, effect of synthesis conditions on the properties of nanoparticles was studied in details. The synthesis conditions included state of matter, composition, concentration, feed rate and spot of injection of precursors, plasma power and flow rate of carrier and atomization gases, respectively. The SiO_2 and LaB_6 nanopowders have been characterized for particle morphology, specific surface area, bulk and surface chemical composition and phase composition.

Correlations were established among synthesis conditions and properties of nanopowders. It has been proved that RF thermal plasma reactors are effective equipments for synthesizing ceramic nanopowders of special properties.

Keywords: RF thermal plasma; Ceramic nanopowders; Silicon dioxide; Lanthanum hexaboride

1. Introduction

Synthesis and application of nanosized powders of unique properties stood in the limelight of research and development in the last couple of years.[1,2] These materials can be produced by different methods such as sol–gel processing, high-energy ball milling, mechanical attrition, laser ablation, physical and chemical vapour deposition, flame pyrolysis and plasma synthesis.

The "traditional" wet-chemistry methods including sol–gel techniques are capable of producing nanosized powders of controlled size and morphology. However, they cannot be used for mass production because the precursors are expensive, the production rate is low and liquid by-products are generated. Thus, nanosized powders are mostly produced by aerosol processes.[3] In these processes the precursors are heated to high temperatures where they are transformed into gaseous or vapour-phase species from which the targeted molecules are formed in subsequent chemical reactions. The product molecules then coagulate to bigger particles through collisions in the high temperature zone. The primary particles can grow further by coagulation, coalescence or sintering if the reaction conditions allow it. The process is typically realized in a flame reactor which provides sufficient concentration and thermal gradients to prohibit excessive growing of particles. Thermal plasma reactors are also used for this purpose. In thermal plasmas even solid precursors can be evaporated and the products will be nucleated in the nanometre range due to the supersaturation of the vapour phase. The advantages plasma flames can provide over hydrocarbon flames include the ease of power adjustment. The power and consequently the reaction temperature can be independently controlled from the gas composition and flow rate. In thermal plasma case, however, the scaling-up and the precise control of size distribution may be difficult.

In this paper we report on the preparation of two different ceramic nanopowders in RF thermal plasma reactor. The models include (i) synthesis of silica from TES (tetraethyl-silicate) and (ii) synthesis of LaB_6 nanopowders from La_2O_3 and B powders. Selection of particular models was partly reasoned by their practical importance. Silica nanoparticles are applied as additives in the plastic industry, as fillers in rubber production, for catalyst support and in the ceramic industry.[4] Ceramic materials based on lanthanum hexaboride have a low work function of about 2.5 eV. They are applied as hot cathodes in electron microscopes, microwave tubes, electron beam welding machines, X-ray tubes and heat absorbing layers. Another motivation of model selection was that different precursors (liquid and solid, respectively)

* Corresponding author. Tel.: +36 1 4381130; fax: +36 1 4381147.
E-mail address: szepvol@chemres.hu (J. Szépvölgyi).

0955-2219/$ – see front matter © 2007 Elsevier Ltd. All rights reserved.
doi:10.1016/j.jeurceramsoc.2007.09.034

and quite different synthesis conditions were required in the two cases. It allowed to study and to prove the feasibility of thermal plasma reactors in the synthesis of nanosized powders of varying properties.

Synthesis of nanosized silica powders in flame reactors is a well-known and broadly applied production method. Much less information is available on the production of silica nanoparticles in thermal plasma conditions. As far as LaB_6 powder is concerned, only a few papers were published on its synthesis. The most frequent synthesis route of LaB_6 powder involves borothermal reduction of La_2O_3 at 1430–1830 °C, and at reduced pressure.[5,6] There were some studies on the thermal plasma synthesis of LaB_6 powders, as well.[7]

For both models we investigated the effect of key parameters of processing on the properties of products. Particular parameters included state of matter, composition, concentration, feed rate and spot of injection of precursors, plasma power and flow rate of carrier and atomization gases, respectively.

2. Experimental

The experimental apparatus consisted of an RF inductively coupled plasma torch (TEKNA PL 35) connected to a reactor, a cyclone, a filter unit and a vacuum pump. In the silica case the TES precursor (WACKER) was delivered by peristaltic pump (Masterflex) to the atomizer probe placed in the plasma flame. Over there the liquid droplets were atomized and combusted with oxygen gas. The SiO_2 content of TES solutions varied from 14 to 41 m%, while the feed rate changed from 1.6 to 6.2 ml min^{-1}. The plasma torch operated with Ar central gas (15 l min^{-1}) and Ar and O_2 mixed sheath gases (40 and 10 l min^{-1}, respectively) at a constant plate power of 20 kW at nearly atmospheric pressure.

To synthesize LaB_6 nanopowders, a solid mixture of crystalline La_2O_3 (Aldrich) and amorphous B (90 m%, Alfa Aesar) powders was injected axially into the hottest zone of the plasma flame through a water-cooled probe by a PRAXAIR powder feeder. Conditions of LaB_6 synthesis are listed in Table 1.

Thus, the silica nanopowders were synthesized from liquid, while the LaB_6 nanopowders from solid precursors. The two cases involved different evaporation and synthesis routes.

The as synthesized nanoparticles were characterized for particle morphology by SEM (Philips XL30) and TEM (Philips CM20). X-ray diffractometer (Philips PW 1730, CuK_α) was used to analyse the crystalline phases in the products. The specific surface area was measured by nitrogen adsorption at −196 °C on the basis of BET isotherms (Quantachrome, Autosorb-1, five point isotherm). The size distribution of micropores was calculated by the Horváth-Kawazoe (HK) model. The surface chemical composition was studied by XPS (Kratos XSAM 800).

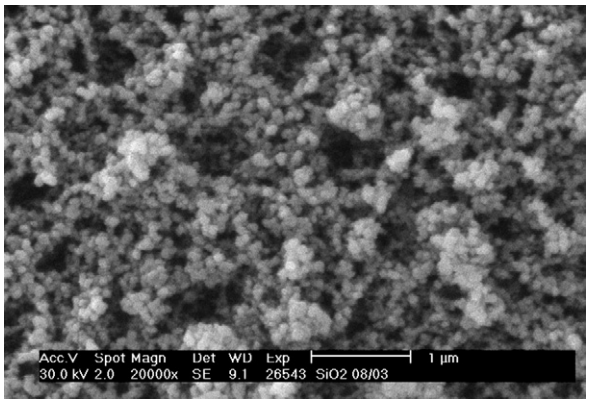

Fig. 1. SEM image of agglomerated silica nanoparticles.

3. Results and discussion

3.1. Synthesis of silica nanoparticles

According to SEM images, spherical nanoparticles were produced (Fig. 1). The primary silica particles have smooth surface, there are neither inner nor surface pores. However, they tend to form agglomerates. The XRD measurements proved that in all cases amorphous silica, actually silica glass was formed with a negligible amount of crystalline material. There was some segregation of silicon on the surface of silica particles: the surface silicon content as determined by XPS measurements was 48.3 m% a bit higher than the stoichiometric value of 46.7 m%. Some carbon contamination was detected on the surface, as well.

The BET specific surface area of silica powders from different tests ranged from 60 to 220 $m^2\,g^{-1}$. Assuming spherical and dense particles (which are the case) the mean particle size can be calculated by the formula of following equation:

$$d_{BET} = \frac{6}{(\rho \cdot SSA)} \quad (1)$$

where SSA is the measured specific surface area and ρ is the density of silica (2.2 g cm^{-3}). Mean particle size of silica grains

Table 1
Conditions and results of LaB_6 synthesis

Run No.	Precursors	Gases (l min^{-1})			E_{spec} [kWh g^{-1}]	R_{XRD}[a]
		Sheath	Plasma	Carrier		
1	La_2O_3 + 20B	Ar-40	Ar-15	H_2-5.85	2.45	18
2	La_2O_3 + 20B	Ar-35; H_2-5	Ar-11; He-5	Ar-1.8	2.23	19.3
3	La_2O_3 + 20B	Ar-35; He-20	Ar-5.7; He-15	He-3.8	1.93	24.7
4	La_2O_3 + 20B	Ar-37; He-3	He-15	Ar-1.8	1.71	37
5	La_2O_3 + 20B	Ar-20; He-28	Ar-11; He-8	He-6	0.78	No La_2O_3

[a] XRD reflection of LaB_6 at $d = 2.94$ related to the reflection of La_2O_3 at $d = 2.28$.

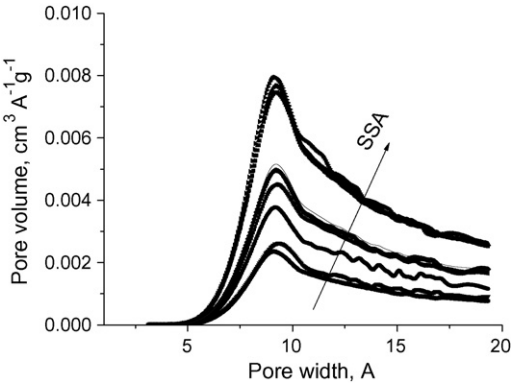

Fig. 2. Porosity of agglomerated silica powders.

formed in these tests ranged from 12 to 42 nm. It is in a good agreement with the results of SEM investigations.

In the given case values of microporosity calculated by the HK model are associated with the pores between the agglomerated particles. It is supported by the finding that the diameter of micropores was 0.9 nm for all samples (Fig. 2). Their amount (i.e. the pore volume) increased with SSA (i.e. decreasing particle size) indicating a greater number of inter-particle holes within the agglomerates (Fig. 2).

A linear relation was observed between the specific surface area and feed rate of precursor at constant values of other variables (Fig. 3). Increase of solution feed rate from 1.7 to 3.6 g·min^{-1} decreases the specific surface area from 220 to 106 m^2 g^{-1} (and increases the particle size from 12 to 26 nm). At higher feed rate the number of product molecules and clusters in a given volume unit, i.e. their volume concentration increases. Thereby, the collision frequency also increases between the molecules that leads to enhanced growth of grains.

The specific surface area of silica nanopowders was depended on the flow rate of atomization gas which determined the atomization efficiency of precursor, as well. Although the correlations among synthesis parameters and specific surface areas or particle sizes are different, the mechanism by which the SSA is affected is more or less common. For these reason we could develop a more general correlation by which one can assess the size of the product particles at different sets of the variables, since all

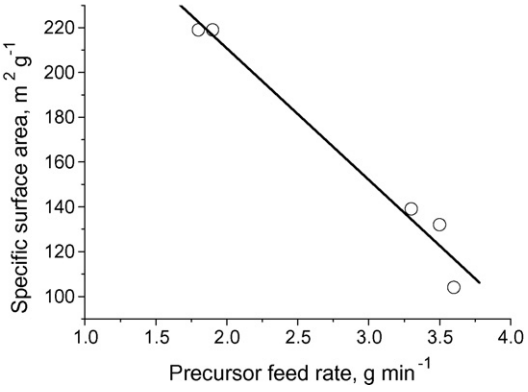

Fig. 3. Effect of the precursor feed rate on the specific surface area of silica nanoparticles.

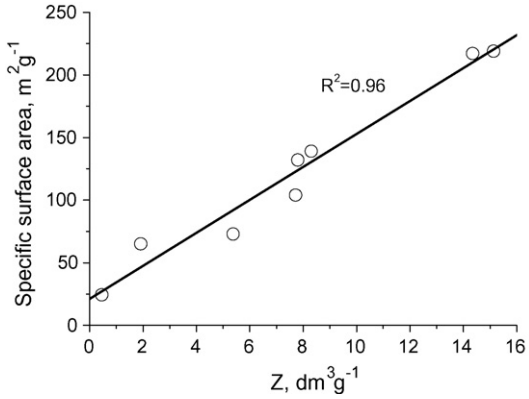

Fig. 4. Correlation between the specific surface area of silica nanoparticles and variable *Z*.

investigated variables can be reduced to a new variable defined as follows:

$$Z = \frac{100 \cdot v}{c \cdot m_f} \quad (2)$$

where Z is the new variable (dm^3 g^{-1}), v is the flow rate of atomization gas (dm^3 min^{-1}), c is the SiO_2 content of TES (m%) and m_f is feed rate of TES solution (g min^{-1}). In physical terms variable Z can be interpreted as the invert of SiO_2 concentration in the atomization gas.

The SSA was plotted against Z in Fig. 4. A linear correlation with good fitting was found between Z and SSA. It confirms the importance of the atomization efficiency of precursor in terms of particle size of products.

3.2. Synthesis of LaB_6 nanoparticles

Conditions and results of LaB_6 synthesis are listed in Table 1 where E_{spec} stands for the energy of RF thermal plasma synthesis related to unit feed of La_2O_3. As it was mentioned above, La_2O_3 powder and boron powder were used as precursors. In Run Nos. 1–5 (Table 1) more or less LaB_6 was formed in all cases. The highest conversion was achieved in Run No. 5 when actually all La_2O_3 was transformed into LaB_6. The diffractogram of particular sample (Fig. 5) precisely suits to the diffraction pat-

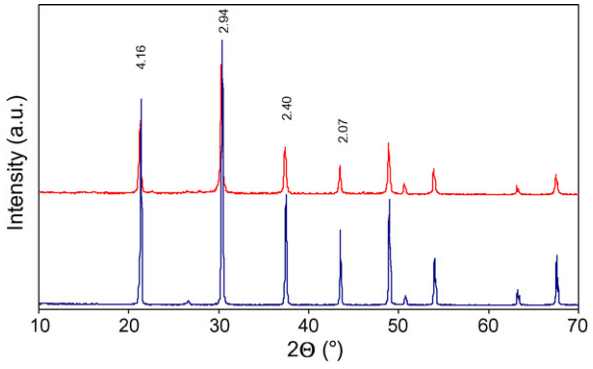

Fig. 5. X-ray diffractogram of commercial LaB_6 sample (lower line) and sample from Run No. 6 (upper line), respectively. Most intense reflections of LaB_6 are labelled.

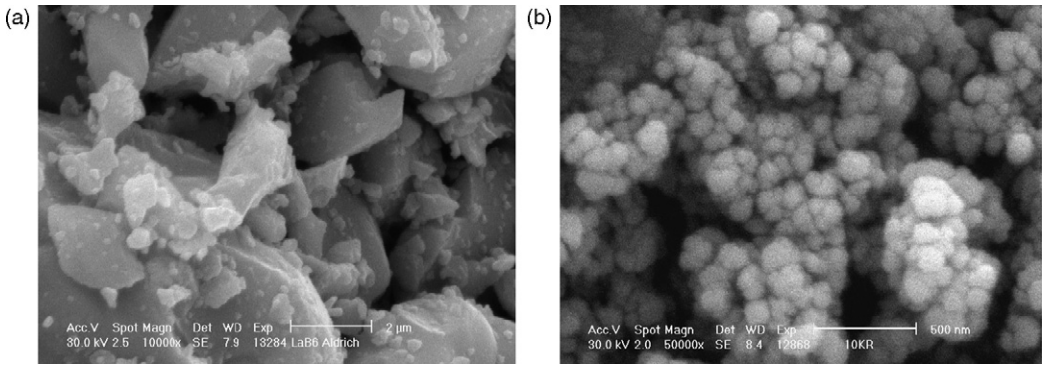

Fig. 6. SEM micrograph of the commercial LaB_6 powder (a) and the thermal plasma powder from Run No. 5 (b), respectively.

terns of commercial LaB_6 powder (Aldrich, <10 μm) selected as reference one.

In spite of the limited number of experiments, some definite tendencies can be established concerning the effect of synthesis conditions on the yield and properties of LaB_6. Addition of helium and/or hydrogen into the sheath and/or plasma and/or carrier gases improves the conversion of La_2O_3 to LaB_6. Our results suggest that for higher conversions, concentration of helium and/or hydrogen should be increased in the gas mixture (Run Nos. 4 and 5). Helium and hydrogen have higher thermal conductivity than argon. They improve the heat transfer between the plasma flame and the solid particles. Thus, higher heating rates and most probably higher reaction temperatures are achieved in their presence that leads to higher LaB_6 yields.

In conditions of present work, nanosized LaB_6 particles were formed which tended to agglomerate in more or less extent (Fig. 6). Fig. 6 reveals that in RF thermal plasma nanoparticles with mean particle size of 10–50 nm are formed contrary to the micron-sized commercial powder. The specific surface area (SSA) of LaB_6 nanopowders varied in the range of 12 to 68 $m^2\,g^{-1}$. Assuming spherical and dense LaB_6 particles (Fig. 6 supports this assumption) the mean particle size of powder with an SSA of 40 $m^2\,g^{-1}$ as calculated by Eq. (1) is 16 nm. It agrees well with the results of SEM investigations.

Surface composition of LaB_6 particles was determined by X-ray photoelectron spectroscopy (XPS). With the XPS MultiQuant code developed in our institute[8,9] thicknesses of surface atomic layers can be calculated from the line intensities, assuming spherical grains. The layered structures calculated from the XPS results are shown in Fig. 7.

The calculated and measured compositions were correctly fitted by assuming that the LaB_6 particles are covered with a

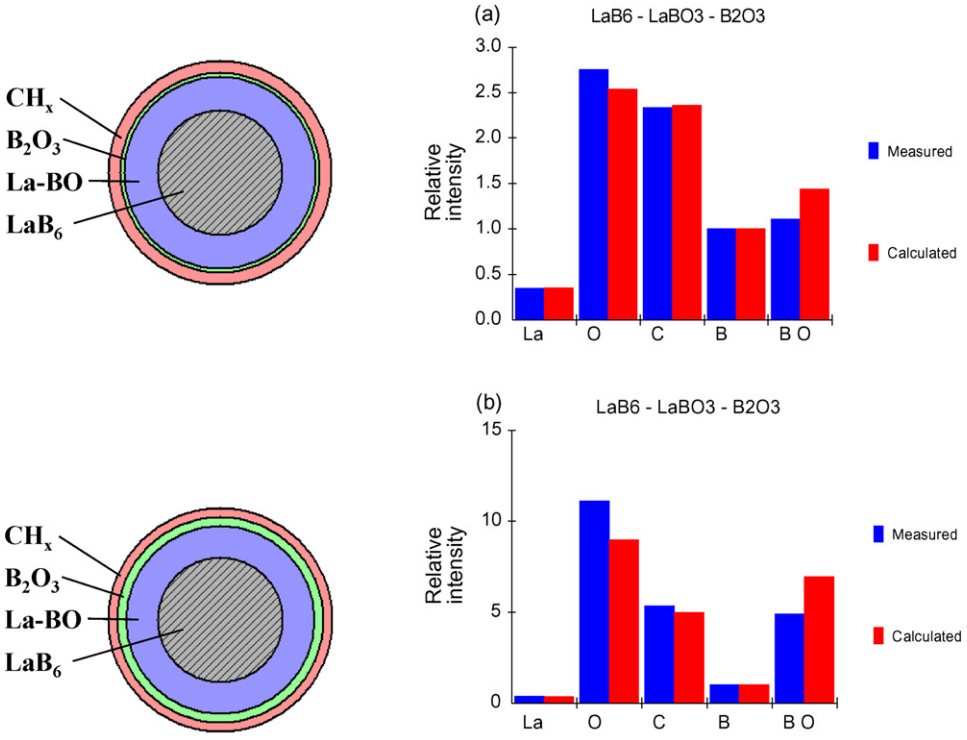

Fig. 7. Layered structure of LaB_6 particles simulated on the basis of XPS analyses for the commercial LaB_6 material (a) and the product from Run No. 5 (b), respectively.

Table 2
Layer thicknesses calculated by the XPS MultiQuant code

Sample	Layer thickness (nm)		
	CH_x	B_2O_3	$LaBO_3$
LaB_6 (Aldrich)	0.85	0.24	2.24
Run No. 5	0.82	1.36	2.66

$LaBO_3$ layer, then a B_2O_3 layer. The outermost surface layer is CH_x which can be found in all samples contacted with ambient air. The calculated layer thicknesses are listed in Table 2. Thickness of B_2O_3 layer is greater in the plasma synthesized powder which can be reasoned by the high excess of boron in the starting mixture. The non-reacted boron particles were quickly oxidized while handling the LaB_6 powder in air.

4. Conclusions

Nanosized silica particles were prepared by combustion of TEOS in an RF thermal plasma reactor. Particles prepared by this way were more or less agglomerated with primary particle size of 12–42 nm. It was found that the particle size can be controlled either with varying the precursor feed rate or the flow rate of atomization gas or the precursor concentration. The lower feed rate, the lower concentration of the precursor solution, as well as the higher flow rate of atomization gas all increase the specific surface area and accordingly reduce the particle size. Introducing a new variable enabled us to establish a good correlation for the specific surface area by means of which the specific surface area can be predicted for different synthesis conditions.

During synthesis of LaB_6 nanopowders high LaB_6 yield was observed at a B/La_2O_3 molar ratio of 20, at plate power of 30 kW, in an Ar/He plasma of >30% He content. A bluish powder was produced which consisted of mainly crystalline LaB_6 particles having a mean size of 10–50 nm. Surface of LaB_6 particles was oxidized due to contact with ambient air.

Acknowledgements

This work has been supported by OTKA Grant T047360, and GVOP Grant 3.1.1-2004-05-0031/3.0.

References

1. Schoonman, J., *Solid State Ionics*, 2000, **135**, 519.
2. Karthikeyan, J., Berndt, C. C., Tikkanen, J., Wang, J. Y., King, A. H. and Herman, H., *Nanostruct Mater*, 1997, **8**, 61.
3. Pratsinis, S. E., *Prog Energy Combust Sci*, 1998, **24**, 197.
4. Wendelin, J., Stark, C. and Pratsinis, S. E., *Powder Technol*, 2002, **126**, 103.
5. Zheng, S., Min, G., Zon, Z., Yu, H. and Zhang, C., *Guisuanyan Xuebao*, 2001, **29**, 2.
6. Zheng, S., Min, G., Zon, Z., Wang, X. and Han, J., *Jinshu Xueabo*, 2001, **37**, 4.
7. Kats, V. I., Palchevskis, E. A., Miller, T. N. and Plotsinya, T. N., *Vysokotemp. Boridy Silitsidy*, Nauka, Kiev, 1982, p. 125.
8. Mohai, M., *Surf Interface Anal*, 2004, **36**, 805.
9. Mohai, M., *Surf Interface Anal*, 2004, **36**, 828.